Physikalisch-Technische Bundesanstalt
Braunschweig and Berlin
National Metrology Institute

Techniken zur Echoreduktion bei Antennenmessungen

Echo reduction techniques in antenna measurements

David Ulm, WG 2.21

Physikalisch-Technische Bundesanstalt

News

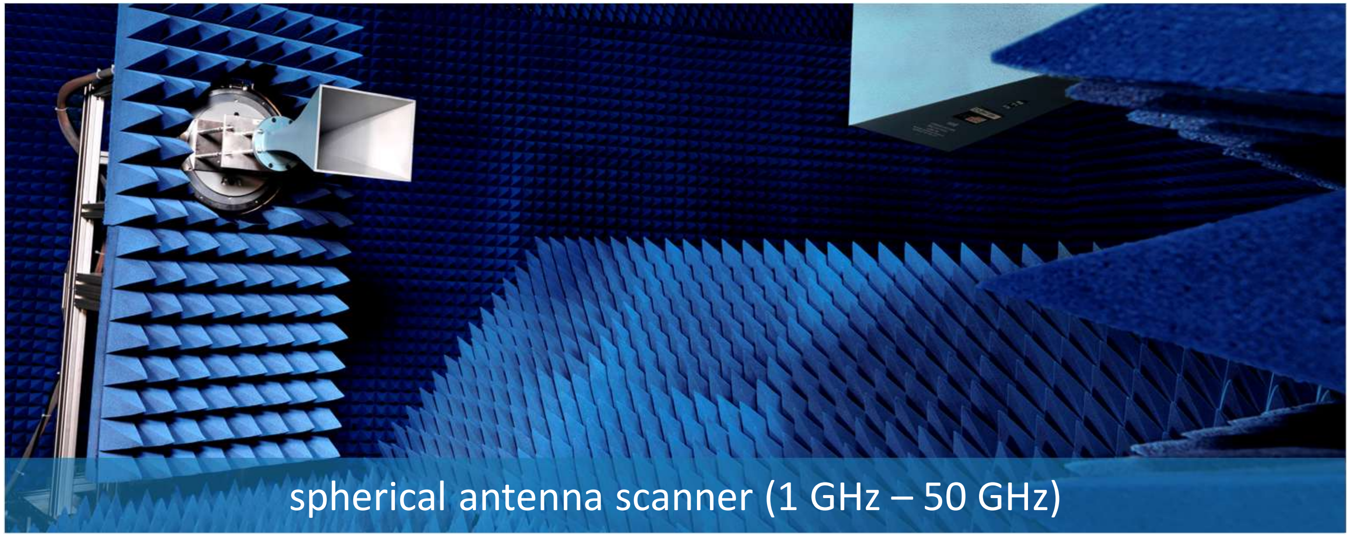
spherical antenna scanner (1 GHz – 50 GHz)


alignment and calibration

- CMC entry requested for antenna gain up to **50 GHz**
- metrological traceability of the coordinates is achieved with the aid of a laser tracker

- *research topic* planar mm-wave scanner: successfully used for near-field measurements up to 170 GHz

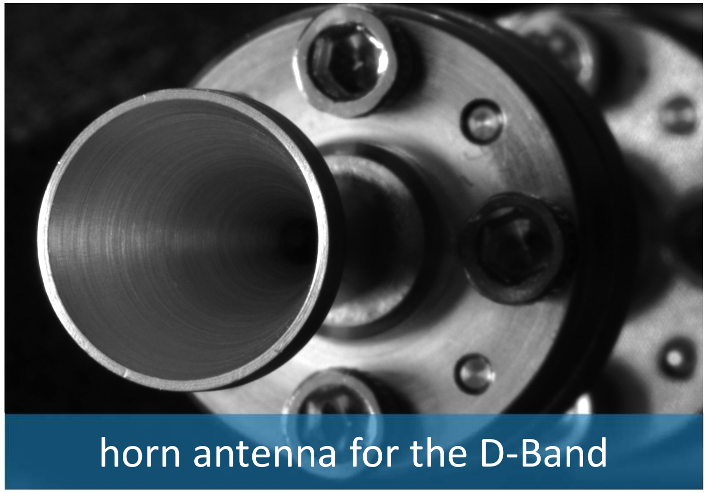
horn antenna for the D-Band

Content

1. Background knowledge
2. Reconstruction of scattering centers
3. Use of a virtual antenna array
4. Mode filtering

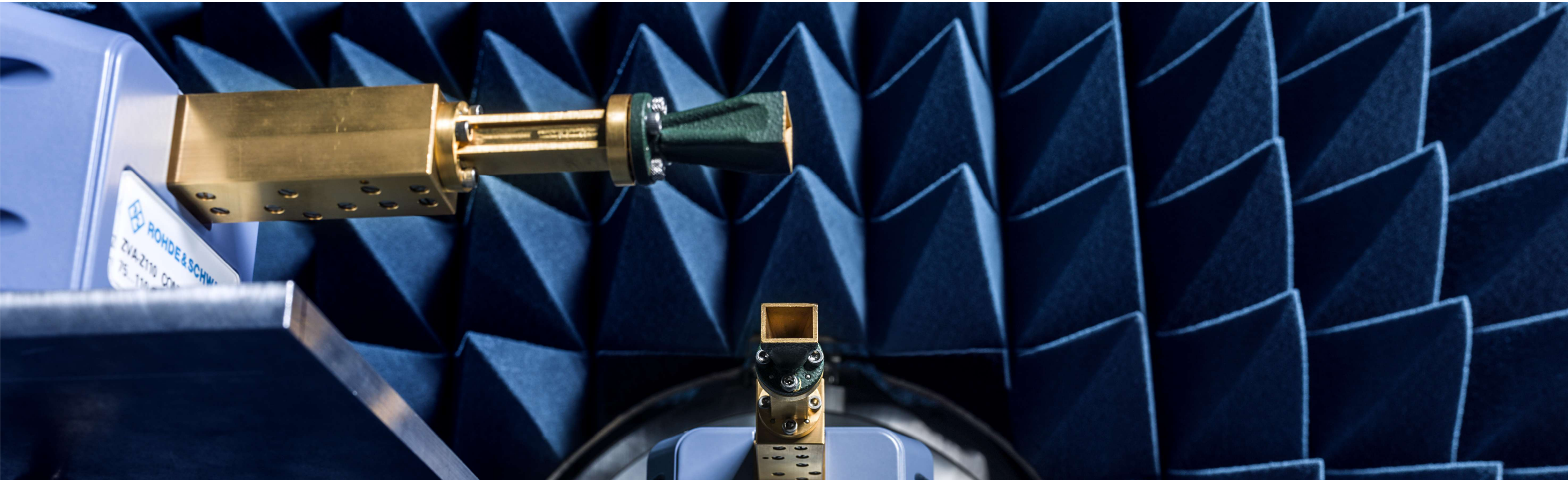

Introduction

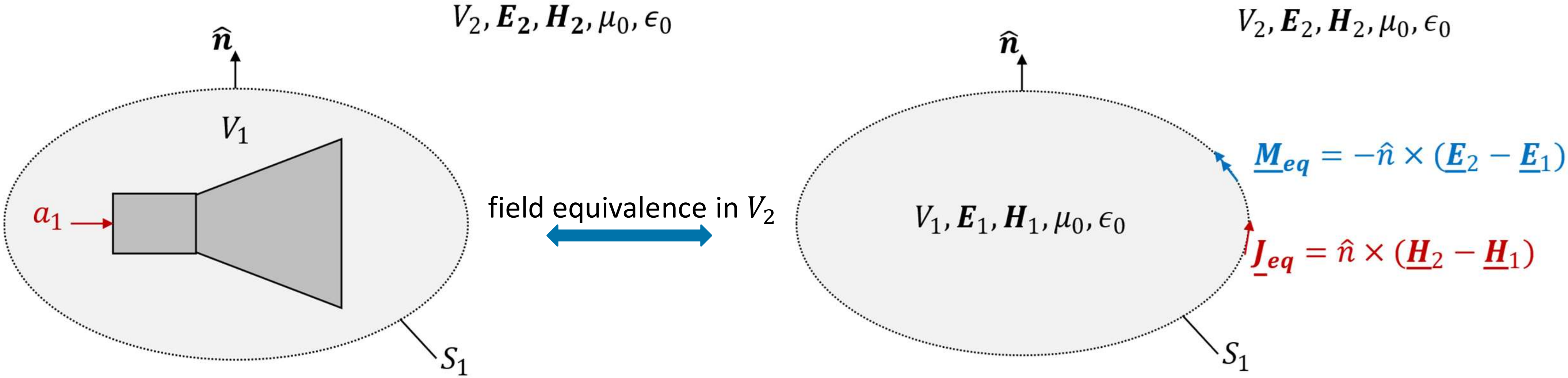

Electric field strength as a superposition of (transversal-electric) plane waves [4.1]:

$$\frac{\boldsymbol{E}(\boldsymbol{r})}{a_1} = -\frac{\mathrm{j}\omega\mu_0}{4\pi} \oiint T_L(\boldsymbol{k}, \boldsymbol{r}) \cdot \tilde{\boldsymbol{w}}_1(\hat{k})\,\mathrm{d}\hat{k}$$

$$= \frac{1 - s_{11}}{I_1\sqrt{Z_0}} \cdot \left[\left(\boldsymbol{I} - \hat{k}\hat{k}\right) \oiint_{S_1} \underline{\boldsymbol{J}}_{eq}(\boldsymbol{r}') \cdot \mathrm{e}^{-\mathrm{j}\boldsymbol{k}\cdot(\boldsymbol{r}_s' - \boldsymbol{r}')}\,\mathrm{d}a' - \frac{\hat{k}}{Z_F} \oiint_{S_1} \underline{\boldsymbol{M}}_{eq}(\boldsymbol{r}') \cdot \mathrm{e}^{-\mathrm{j}\boldsymbol{k}\cdot(\boldsymbol{r}_s' - \boldsymbol{r}')}\,\mathrm{d}a' \right]$$

[4.1] Thomas F. Eibert, Emre Kilic, Carlos Lopez, Raimund A. M. Mauermayer, Ole Neitz, and Georg Schnattinger, "Electromagnetic Field Transformations for Measurements and Simulations (Invited Paper)," Progress In Electromagnetics Research, Vol. 151, 127-150, 2015.

Plane-wave expansion

By using the plane-wave expansion

$$\mathrm{e}^{\mathrm{j}\boldsymbol{kr}} = 4\pi \sum_{\ell=0}^{\infty} \sum_{m=-\ell}^{\ell} \mathrm{j}^{\ell} \cdot \underbrace{j_\ell(kr)}_{\to\, 0,\ \text{for}\ kr \ll \ell} Y_\ell^{m*}(\hat{r}) \cdot Y_\ell^{m}(\hat{k})$$

it can be seen, that the cartesian components of the spectrum of plane waves may be expanded using spherical harmonics Y_ℓ^m [5.1]:

$$\widetilde{\boldsymbol{w}}(\hat{k}) \approx \boldsymbol{T}(\hat{k}) \sum_{\ell=0}^{N} \sum_{m=-\ell}^{\ell} Y_\ell^m(\hat{k}) \cdot \boldsymbol{f}_{\ell m} \quad \text{with: } N = k\frac{d}{2} + n_{buf}$$

- the larger the diameter d of the enclosing minimum sphere of an antenna, the more flexible the pattern

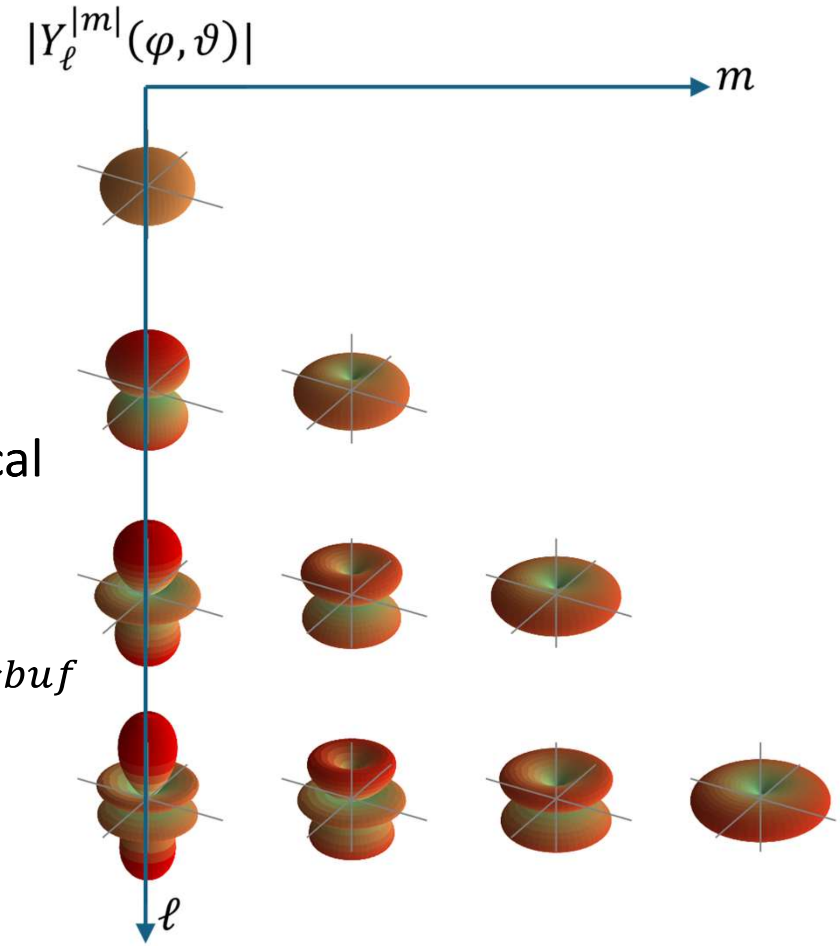

[5.1] T. F. Eibert, D. Ostrzyharczik, J. Kornprobst and J. Knapp, "Solution of Inverse Source Problems with Distributed Spherical Harmonics Expansions," 2022 3rd URSI Atlantic and Asia Pacific Radio Science Meeting (AT-AP-RASC), Gran Canaria, Spain, 2022, pp. 1-4, doi: 10.23919/AT-AP-RASC54737.2022.9814176.

Measurement setup

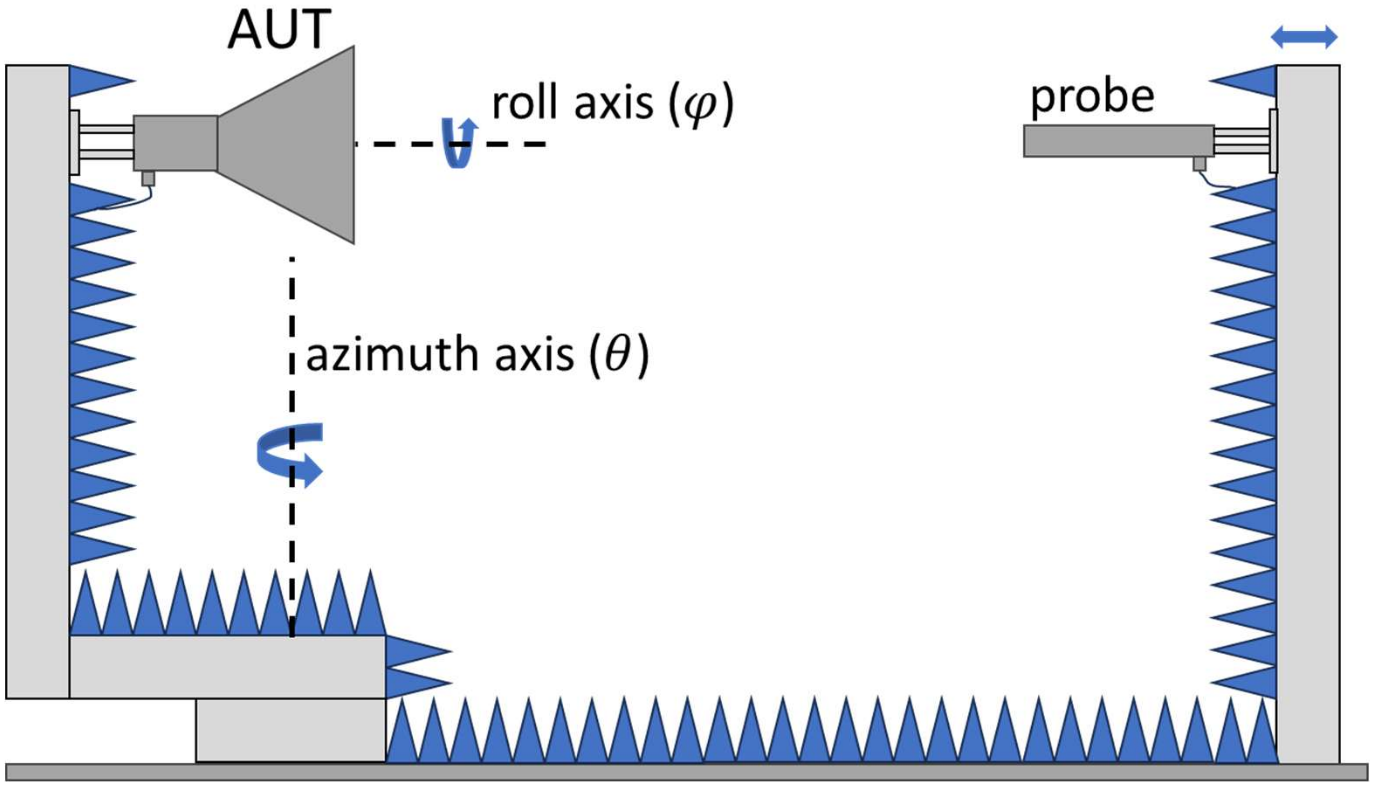

- up to 50 GHz we use a roll-over-azimuth-scanner; the distance between AUT and probe can be varied
- the methods shown here can be adapted accordingly for other scanner geometries

Probe correction

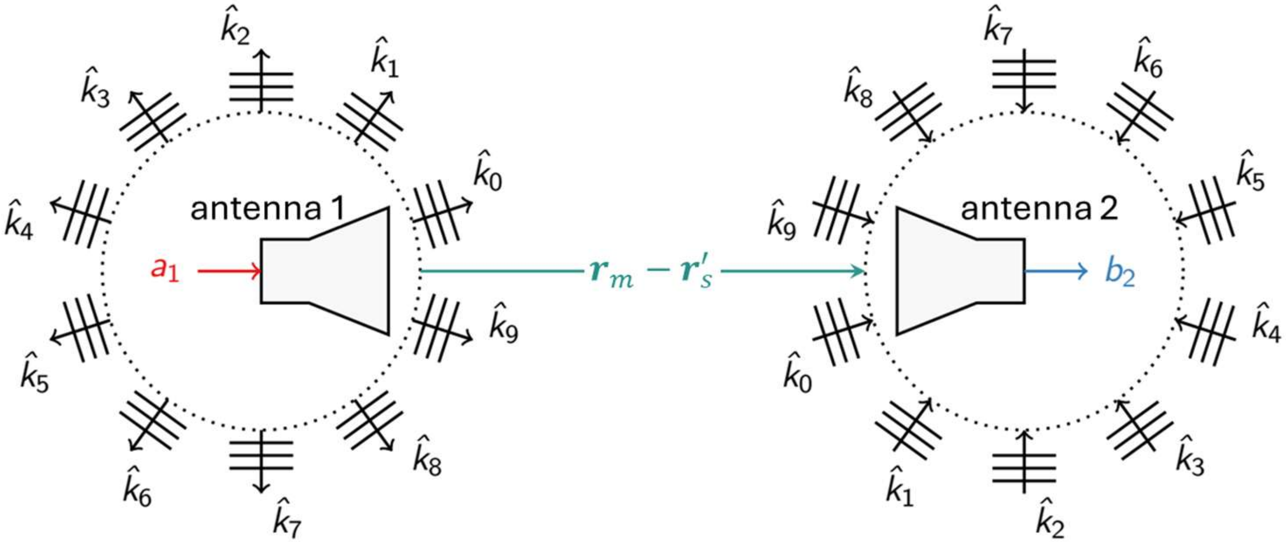

The receiving antenna weights the incident plane waves according to its own antenna characteristics $\tilde{\boldsymbol{w}}_2(-\hat{k})$ [7.1]:

$$\underbrace{s_{21}(\boldsymbol{r}_m)}_{\text{known}} = \frac{\mathrm{j}\omega}{8\pi} \oiint \underbrace{\tilde{\boldsymbol{w}}_2(-\hat{k}) \cdot T_L(\boldsymbol{k}, \boldsymbol{r}_m - \boldsymbol{r}'_s)}_{\text{known}} \cdot \underbrace{\tilde{\boldsymbol{w}}_1(\hat{k})}_{\text{unknown}} \mathrm{d}\hat{k} \xrightarrow{\text{discretization}} \boldsymbol{s}_{21} = \frac{\mathrm{j}\omega}{8\pi} \cdot \boldsymbol{C} \cdot \tilde{\boldsymbol{f}}_1$$

[7.1] D. Ulm, T. Kleine-Ostmann and T. Schrader, "Antenna calibration based on near-field to far-field transformation algorithms," 2019 13th European Conference on Antennas and Propagation (EuCAP), Krakow, Poland, 2019, pp. 1-4.

Content

1. Background knowledge
2. Reconstruction of scattering centers
3. Use of a virtual antenna array
4. Mode filtering

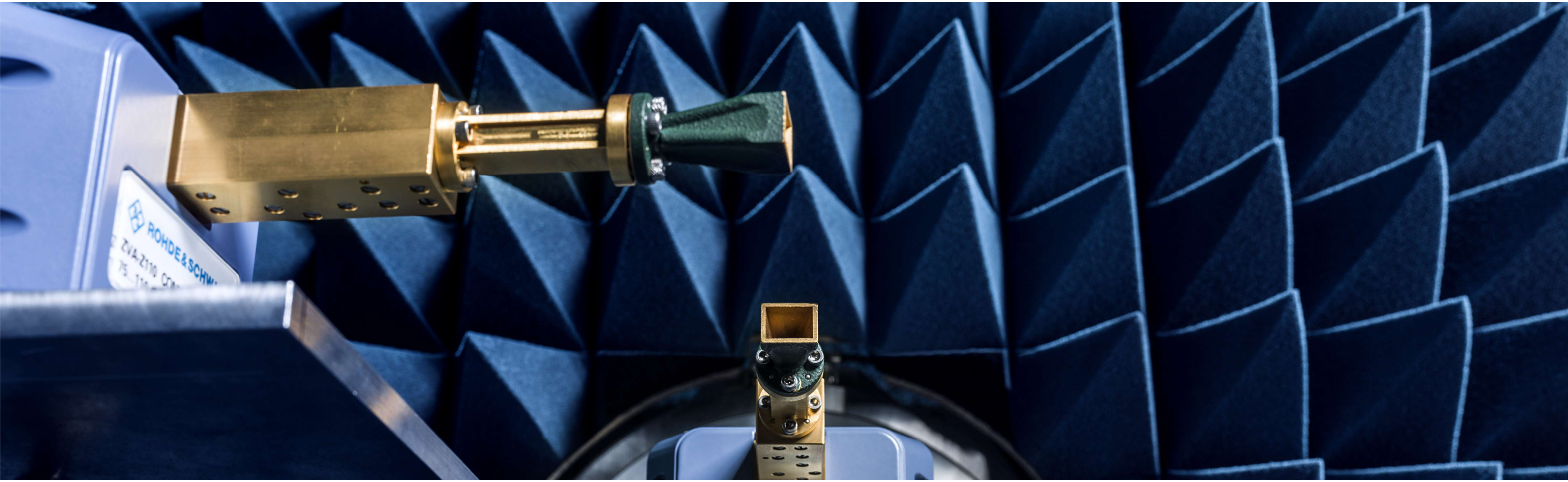

Modeling of scattering centers

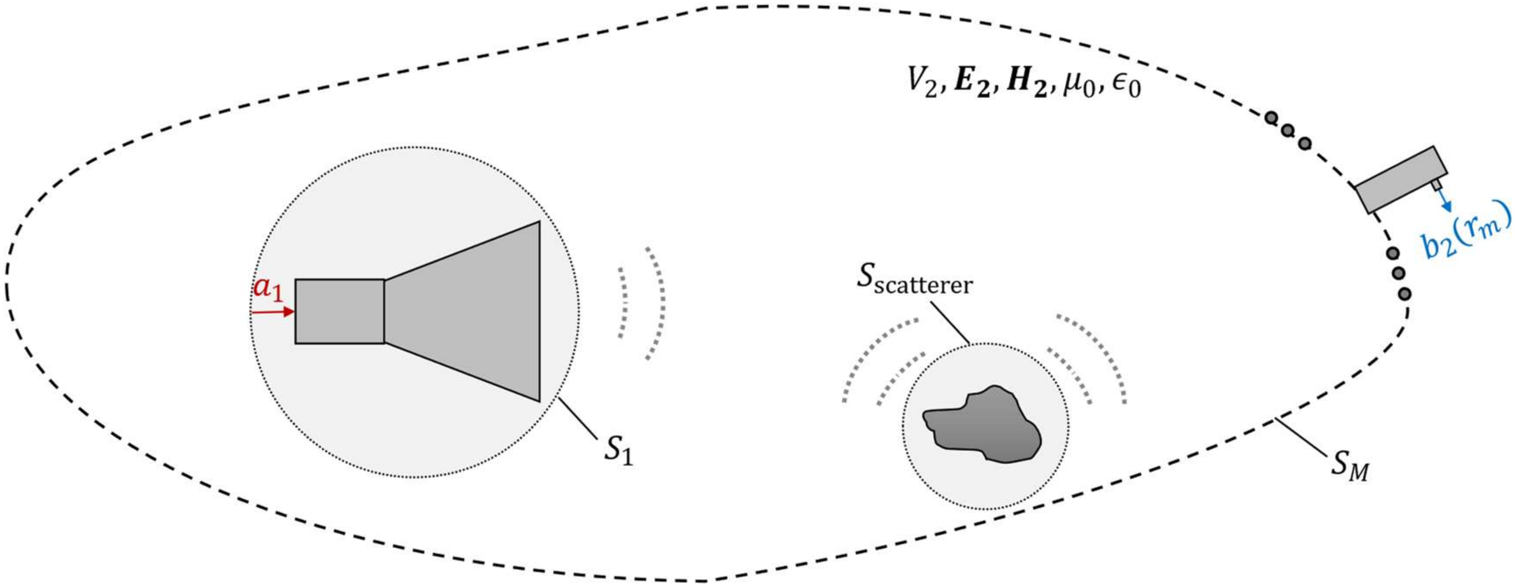

For fixed AUTs, the influence of additional scatterers may be modelled as additional sources:

$$\boldsymbol{s_{21}}(\boldsymbol{r_m}) = \frac{b_2(\boldsymbol{r_m})}{a_1} = \sum_i \oiint \widetilde{\boldsymbol{w}}_{\mathbf{Probe}}\left(-\hat{k}\right) \cdot T_L(\boldsymbol{k}, \boldsymbol{r_m} - \boldsymbol{r}_i') \cdot \left(\boldsymbol{I} - \hat{k}\hat{k}\right) \widetilde{\boldsymbol{w}}_{\boldsymbol{i}}\left(\hat{k}\right) \mathrm{d}\hat{k}$$

as long as AUT and scatterer are well separated, both can be uniquely determined, with which the radiated fields of the AUT can then be calculated without scatterer [9.1]

[9.1] J. Knapp and T. F. Eibert, "Separating Field Contributions by their Source Volumes: Uniqueness and Limitations," 2023 17th European Conference on Antennas and Propagation (EuCAP), Florence, Italy, 2023, pp. 1-5, doi: 10.23919/EuCAP57121.2023.10133465.

Test scenario – simulated measurement

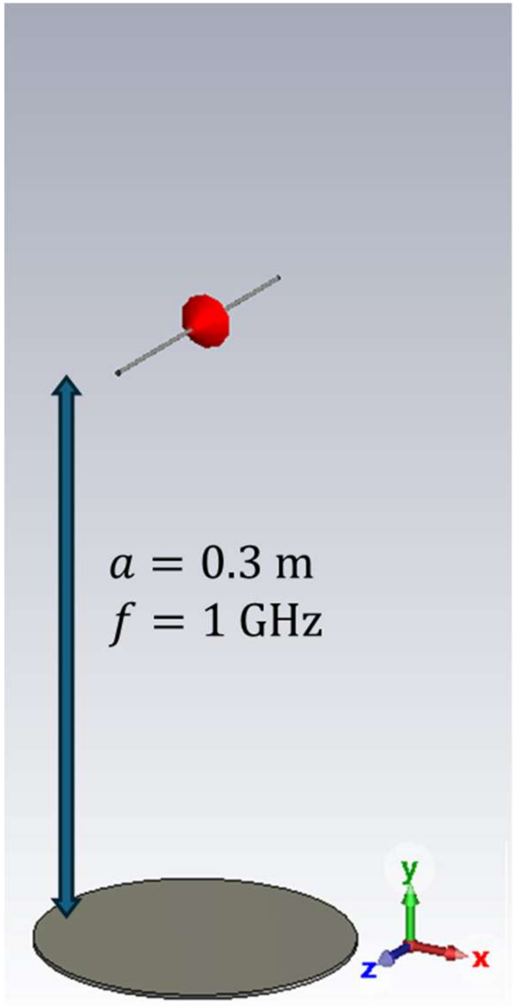

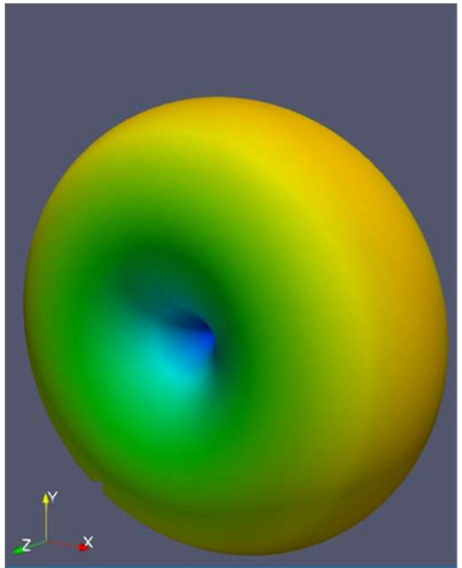

free-space

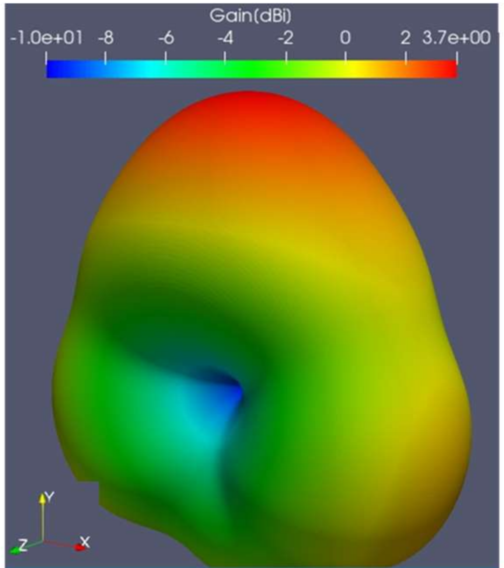

with reflector

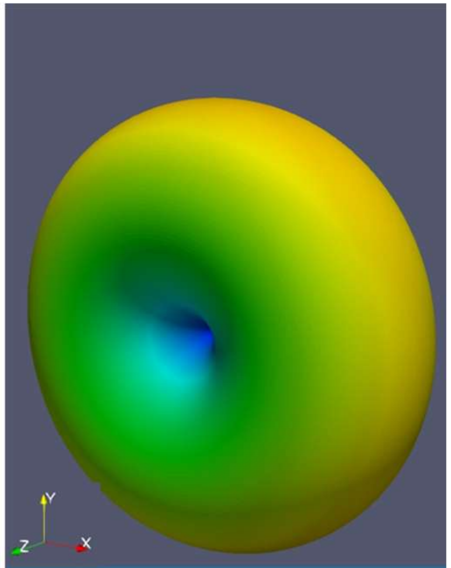

quasi free-space

- in the simplest case, one source sphere is assumed for the AUT and one for the scatterer:

$$\boldsymbol{s}_{21} \approx [\boldsymbol{C}_{\mathrm{AUT}} \quad \boldsymbol{C}_{\mathrm{scatterer}}] \cdot \begin{pmatrix} \boldsymbol{f}_{\mathrm{AUT}} \\ \boldsymbol{f}_{\mathrm{scatterer}} \end{pmatrix}$$

- with the AUT coefficients $\boldsymbol{f}_{\mathrm{AUT}}$, the quasi free-space behavior of the AUT can be calculated

Content

1. Background knowledge
2. Reconstruction of scattering centers
3. Use of a virtual antenna array
4. Mode filtering

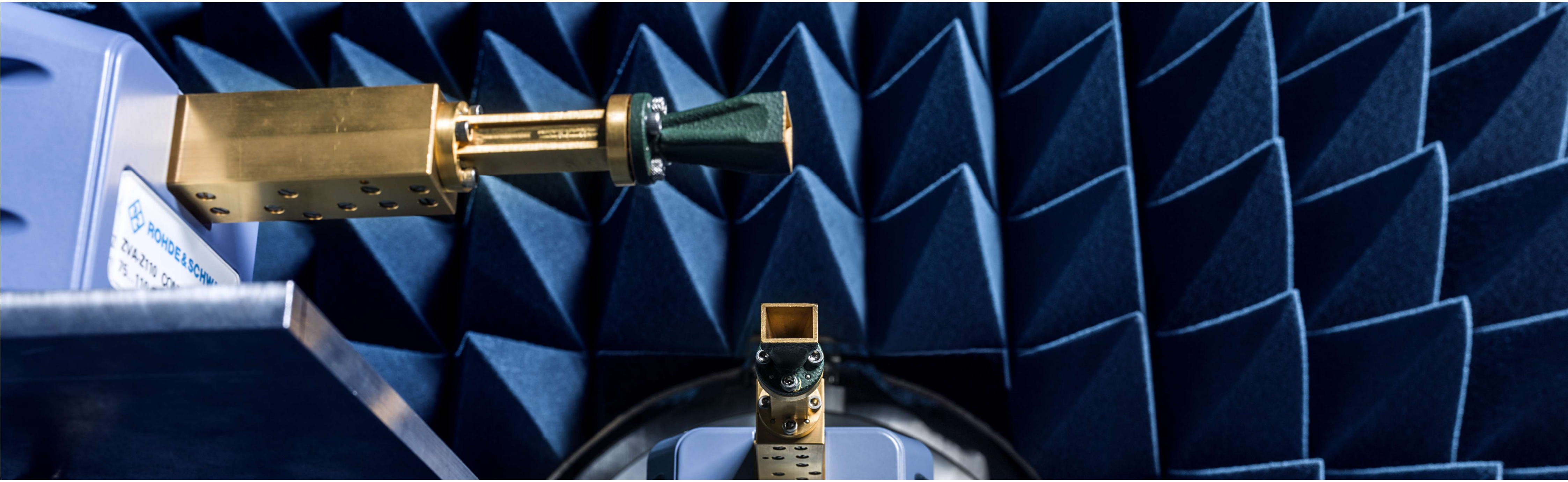

Use of a virtual antenna array

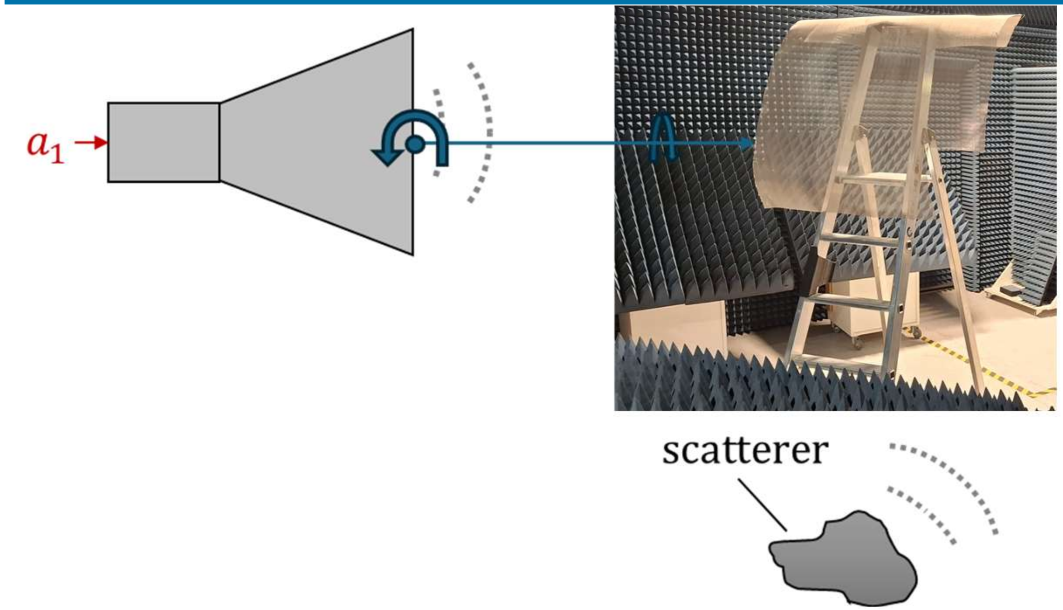

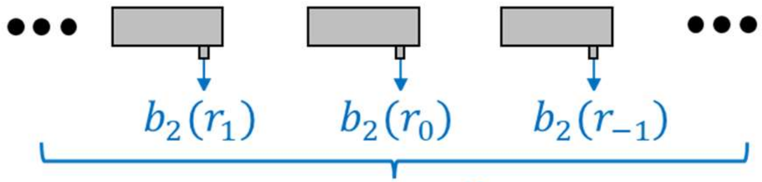

$$b_{2,\,\text{array}}(r_0) = \sum_{n=-N}^{N} a_n \cdot b_2(r_n)$$

$$\tilde{\boldsymbol{w}}_{\text{array}}(\hat{k}) = \tilde{\boldsymbol{w}}_{\text{probe}}(\hat{k}) \cdot AF(\hat{k})$$

- chamber reflections can also be reduced by using a virtual antenna array, particularly in case of a moving AUT [12.1] [12.2]
- since one knows the array factor of the virtual array, one can estimate the suppression of chamber reflections

[12.1] J. Knapp and T. F. Eibert, "Near-Field Antenna Pattern Measurements in Highly Reflective Environments," in IEEE Transactions on Antennas and Propagation, vol. 67, no. 9, pp. 6159-6169, Sept. 2019).
[12.2] Kleine-Ostmann, T. & Ulm, D. & Schrader, T.. (2016). Phase center estimation and correction of multi-path effects for the calibration of mm-wave antennas. 1-2. 10.1109/IRMMW-THz.2016.7758483.

Test scenario – virtual antenna array

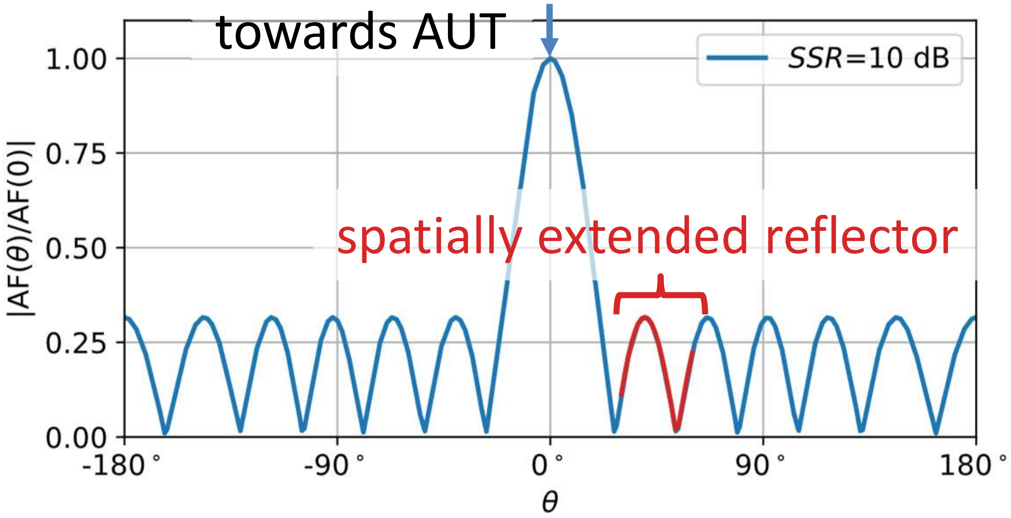

- use of a virtual antenna array with seven elements in highly-reflective environment
- Dolph-Chebyshev weights with a sidelobe suppression ration of 10 dB

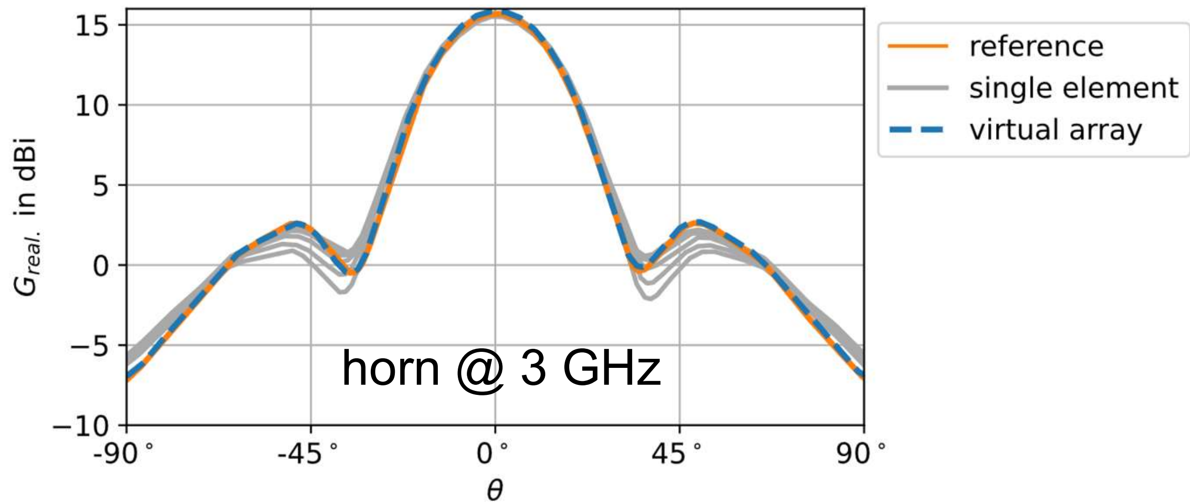

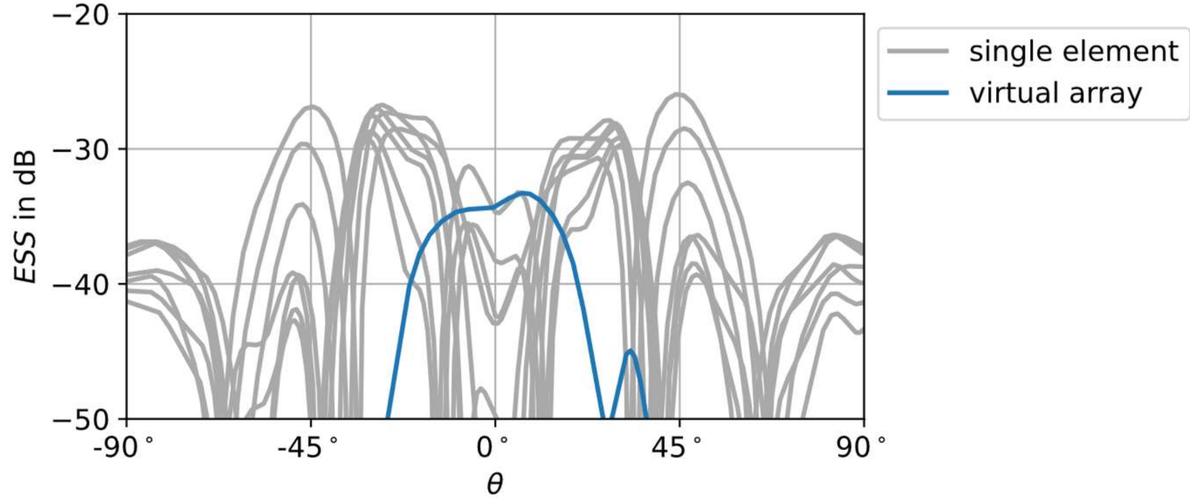

Content

1. Background knowledge
2. Reconstruction of scattering centers
3. Use of a virtual antenna array
4. Mode filtering

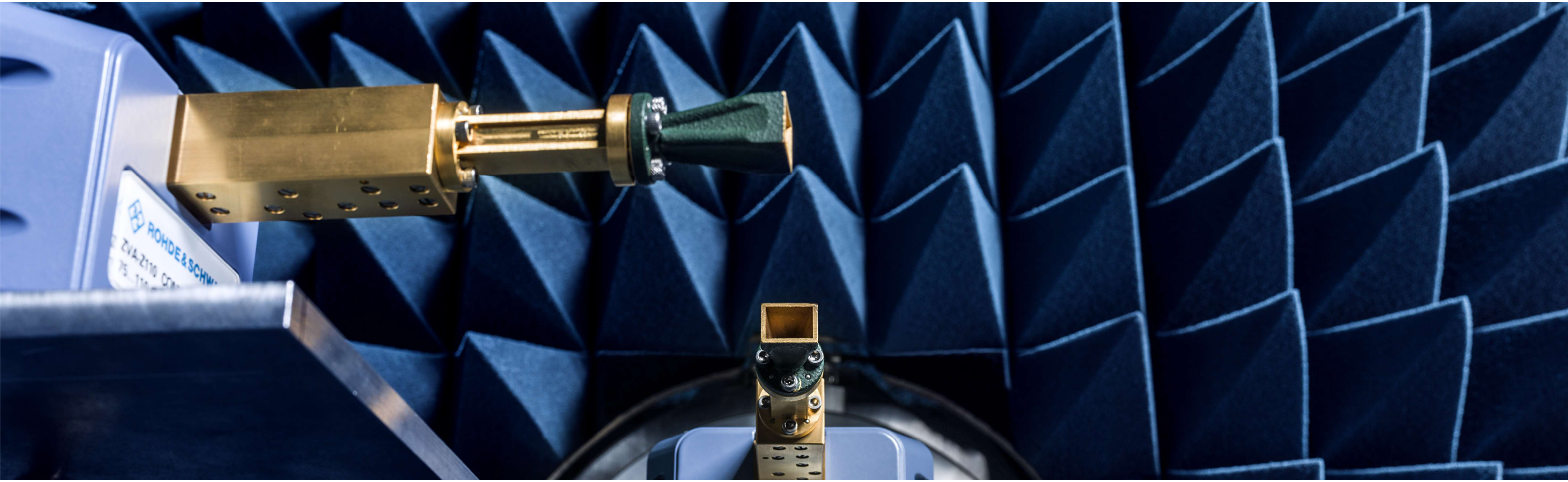

Mode filtering – preliminary consideration

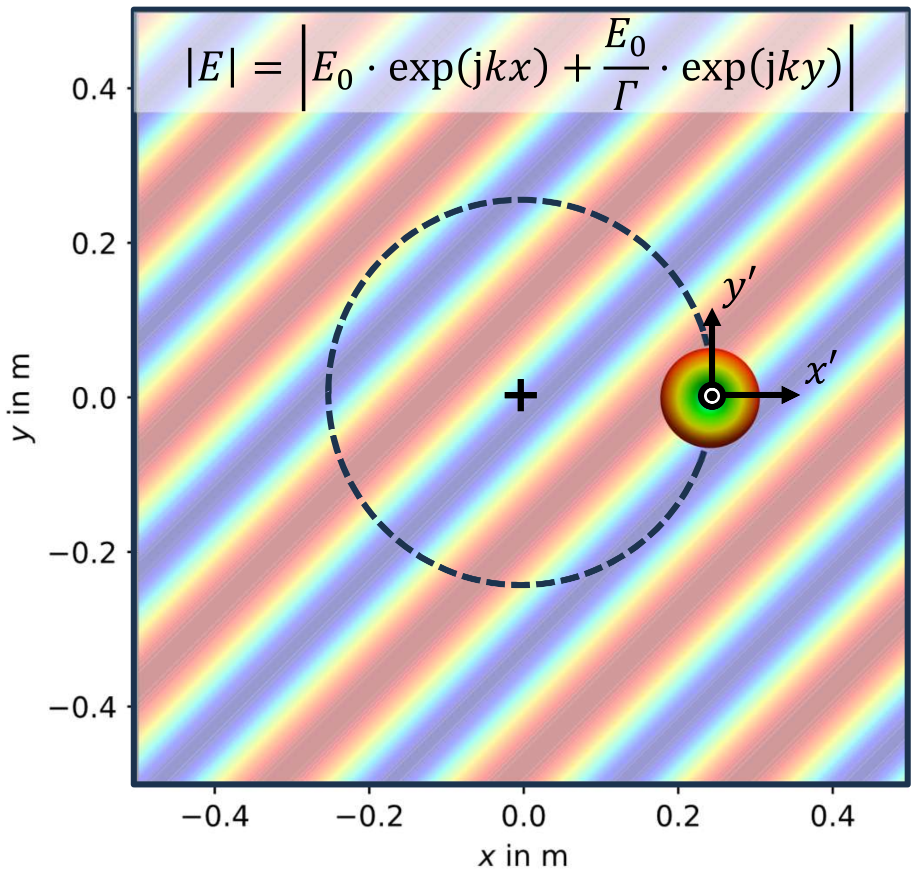

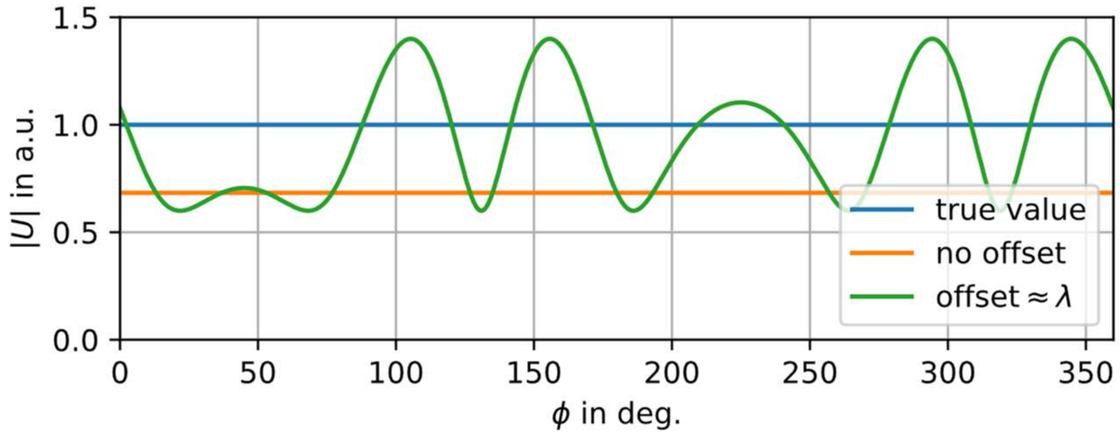

- multipath propagation can lead to interference in the measurement volume

  ▶ displacement of the AUT leads to an angle-dependent oscillating measurement signal

- if the displacement is sufficiently large, this cannot be explained by the antenna

Test scenario – mode filtering

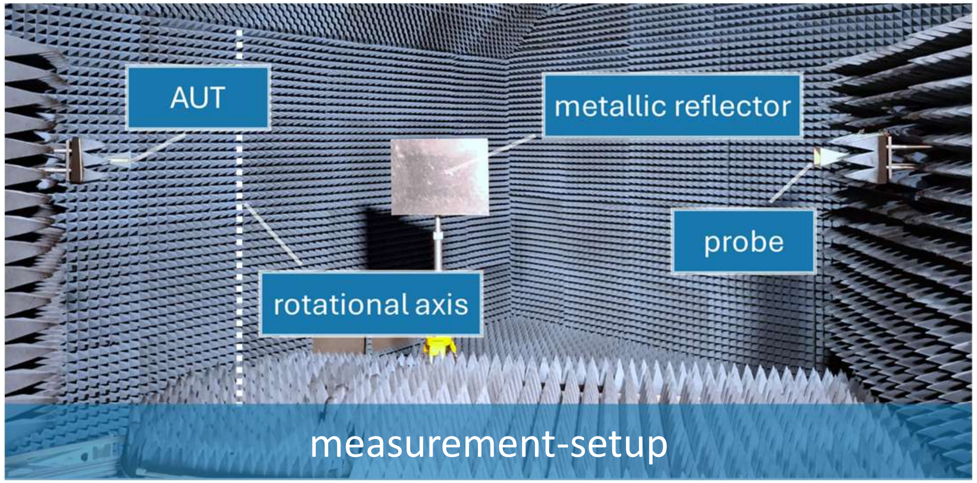

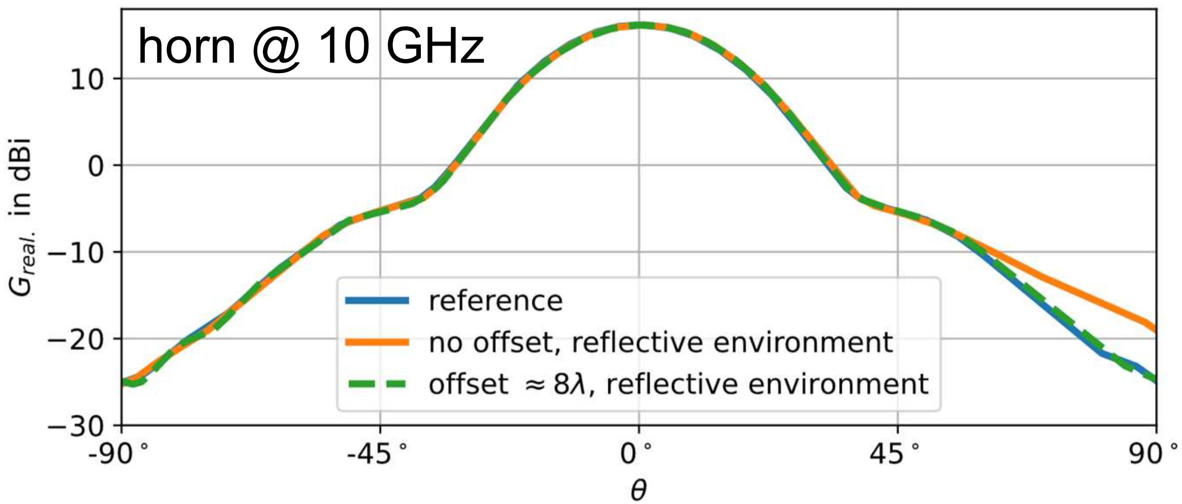

- the (spatial) sampling rate must be increased depending on the displacement in order to avoid aliasing
- the method works particularly well with a spatially strongly varying interference pattern
  - ▶ the angle between the direct wave and the reflected wave must be sufficiently large

- classically, eigenmodes are used instead of scalar spherical harmonics [16.1]

[16.1] Parini, C., Gregson, S., McCormick, J., Van Rensburg, D. J., & Eibert, T. (2021). Theory and practice of modern antenna range measurements: 2nd expanded edition volume 2. in Theory and Practice of Modern Antenna Range Measurements (S. 1-1135). Institution of Engineering and Technology.

Summary – mode filtering

- reflections from the linear stage can be reduced with the aid of an offset mount
- mode filtering can also be used to reduce the uncertainty due to multipath propagation in planar or cylindrical scanner geometries
- further application of mode filtering: far-field measurements [17.1] and assessment of the quality of EMC chambers [17.2]

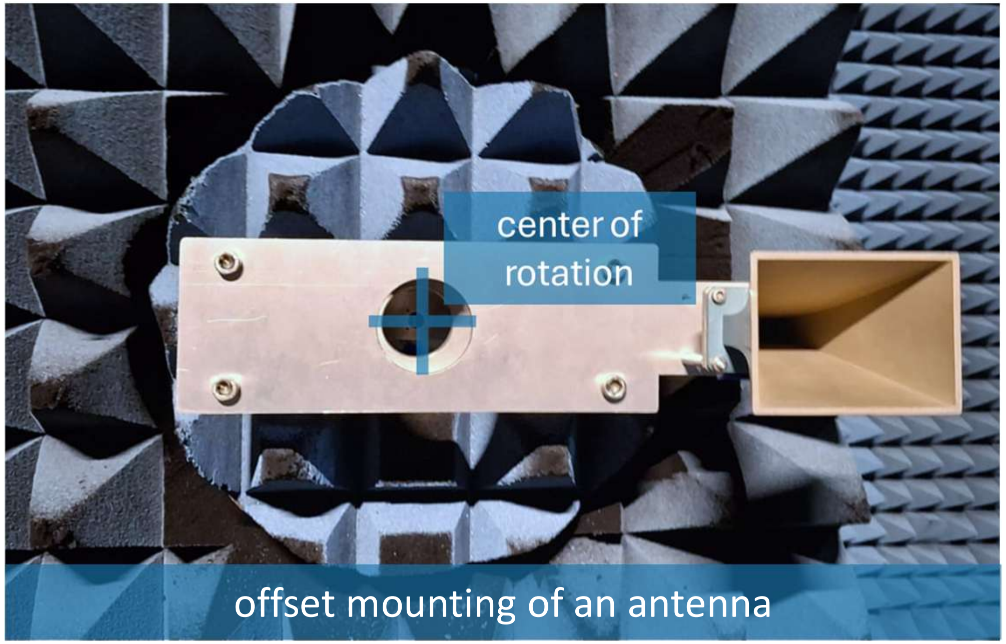

[17.1] Gregson, S. & Newell, Allen C & Hindman, G.. (2012). Examination of Far-Field Mathematical Absorber Reflection Suppression through Computational Electromagnetic Simulation. International Journal of Antennas and Propagation. 2012. 10.1155/2012/623268.

[17.2] Z. Chen and S. Gregson, "Intercomparisons of Site VSWR Measurement Methods using Mode Filtering, Time Domain and Spatial Sampling Techniques," 2021 Antenna Measurement Techniques Association Symposium (AMTA), Daytona Beach, FL, USA, 2021, pp. 1-6, doi: 10.23919/AMTA52830.2021.9620661.

Summary

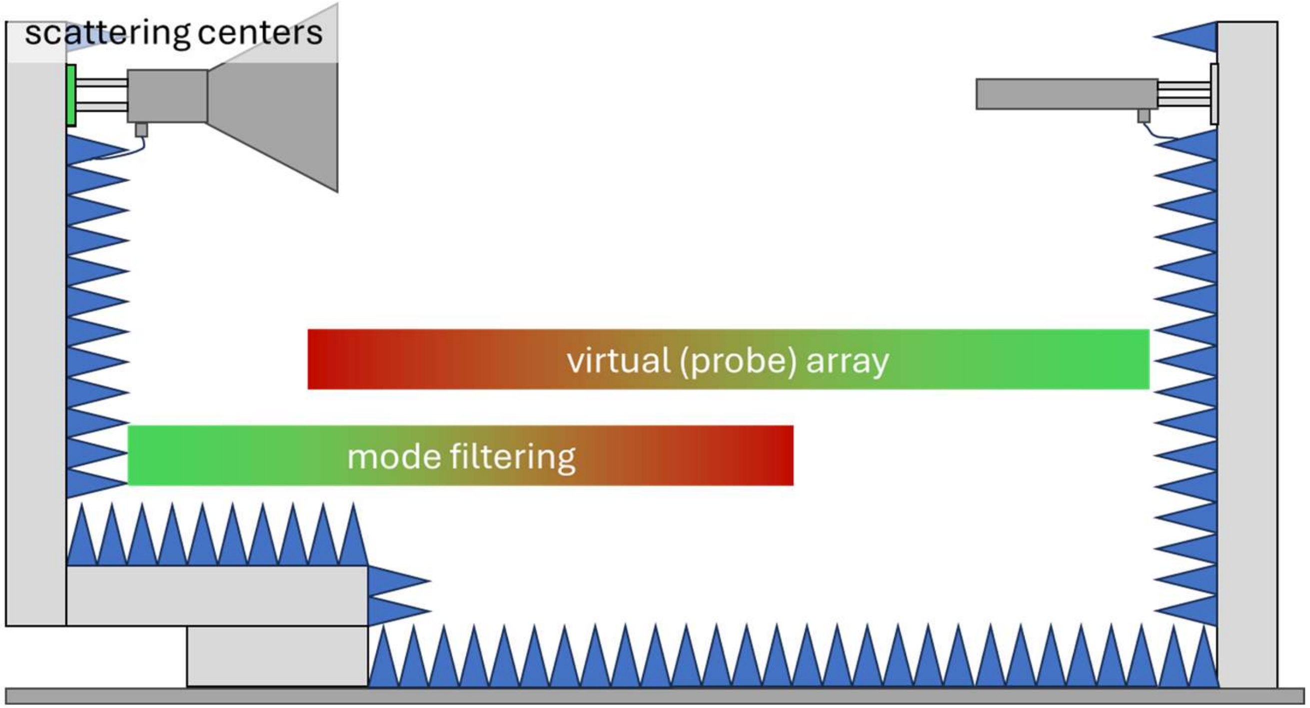

- three methods for the reduction of multipath propagation/echoes were presented
- depending on the location of the reflector, the different methods are more or less suitable
- all methods use geometric a priori information and do not assume a smooth frequency response

Physikalisch-Technische Bundesanstalt
Bundesallee 100
38116 Braunschweig, Germany

David Ulm

Department 2.2 – High Frequency and Electromagnetic Fields

+49 531 592 2214

david.ulm@ptb.de

https://www.ptb.de/cms/ptb/fachabteilungen/abt2/fb-22.html

scan me